Petroleum 5 (2019) 58–66

Contents lists available at ScienceDirect

Petroleum

journal homepage: www.keaipublishing.com/en/journals/petlm

A study of the performance of the LSWA CO_2 EOR technique on improvement of oil recovery in sandstones

H. Al-Abri [a], P. Pourafshary [b, *], N. Mosavat [c], H. Al Hadhrami [d]

[a] Petroleum Development Oman, Oman
[b] Department of Petroleum Engineering, School of Mining and Geosciences, Nazarbayev University, Kazakhstan
[c] Department of Engineering and Technology, Muscat University, Oman
[d] Department of Petroleum and Chemical Engineering, Sultan Qaboos University, Oman

ARTICLE INFO

Article history:
Received 3 May 2018
Received in revised form
25 May 2018
Accepted 4 July 2018

ABSTRACT

Low salinity water is an emerging enhanced oil recovery (EOR) method that causes wettability alteration towards a favorable state to reduce residual oil saturation, while water alternating gas (WAG) is a proven EOR process that enhances oil recovery by controlling mobility of both water and gas. Therefore, combining the two EOR processes as low salinity water-alternating CO_2 EOR injection (LSWA CO_2) can further improve oil recovery by promoting the synergy of the mechanisms underlying these two methods.

Core flooding experiments, contact angle, interfacial tension (IFT), and CO_2 solubility measurement in oil and brine were conducted to investigate the viability and performance of LSWA CO_2 in sandstone reservoirs. A favorable wettability alteration, along with IFT reduction and mobility control, are the mechanisms that contribute to residual oil mobilization efficiencies during the LSWA CO_2 EOR process. In addition, LSWA CO_2 core flooding experiments result in a significant incremental oil recovery.

Three smart waters were tested in our research, to examine the impact of changing cationic composition on oil recovery. The solutions are designed brines as NaCl (SW1), $MgCl_2$ (SW2), and KCl (SW3). Of the three solutions, SW1 yields the highest incremental oil recovery and highest IFT reduction. In addition, it results in a favorable wettability alteration towards a more water-wet state.

In all cases, introducing CO_2 to the brine/oil system shows a great advantage in terms of enhancing wettability modification, promoting IFT reduction, and controlling the displacement front of the injected fluid through mobility control.

1. Introduction

Low salinity/Smart waterflooding is considered to be a tertiary oil recovery technique, in which the composition of the injected brine is modified to achieve the appropriate condition for oil recovery enhancement. Low salinity water (LSW) is usually obtained by diluting high salinity water, while smart water is prepared by selecting active determining ions which are believed to increase oil recovery. Low salinity waterflooding was first recognized in 1990 b y Morrow [1] during experimental work on the effect of the CBR (i.e. crude oil, brine and rock) system on wettability. Different laboratory works have proven that LSW successfully improves oil recovery. For example, the increase in oil recovery from a sandstone reservoir due to injection of low salinity brine was up to 40% as reported by McGuire et al. [2]. LSW has many advantages such as low costs, it is environmentally friendly, and is a simple process to implement compared to chemical EOR methods. It can be used either as a secondary mode or a tertiary mode or with other EOR techniques, such as the polymer flooding and miscible WAG process [3].

The mechanism behind low salinity water flooding has been extensively investigated by many researchers. Since 1990, several

* Corresponding author.
E-mail addresses: hasna.abri@pdo.co.om (H. Al-Abri), peyman.pourafshary@nu.edu.kz (P. Pourafshary), nmosavat@muscatuniversity.edu.om (N. Mosavat), Hadhrami@squ.edu.om (H. Al Hadhrami).

Peer review under responsibility of Southwest Petroleum University.

Production and Hosting by Elsevier on behalf of KeAi

https://doi.org/10.1016/j.petlm.2018.07.003

mechanisms of LSW have been proposed, such as fines migration of detached mixed-wet clay particles with absorbed residual oil drops [4], rock dissolution [5,6], saponification [2,7], cation exchange [8–11], and double layer expansion [12–14]. A combination of these methods leads to the most accepted mechanism, which is wettability alteration [8,15–17]. It has been observed that injection of LSW changes the end points of relative permeabilities [18,19], causing higher relative permeability of the oil and lower relative permeability of the water which indicates that the system has been changed toward water wetness.

The WAG process includes injection of gas into the reservoir, followed by water which acts as a chasing fluid. The number of WAG cycles, slug size, and WAG ratio are determined by the operators. It involves two steps: initially, gas is injected into the reservoir which reacts with the existing crude oil causing oil swelling and reduction in viscosity, thereby increasing the mobility of the oil. Therefore, oil will be displaced from the pores by the gas that cannot be reached by water. Injection water also improves the oil recovery due to the enhancement of viscous force in pores. WAG is used to control water mobility by stabilizing the displacement front during water injection and reducing viscous fingering [20]. In addition, the WAG process reduces the gas override effect during gas injection [21]. Therefore, both microscopic and macroscopic sweep efficiencies are improved through this process.

There are three main WAG parameters that determine the efficiency of this process on oil recovery: WAG slug size, WAG ratio, and WAG cycles. For WAG slug size, the amount of the injected water and gas should be specified carefully, for example injecting too much gas affects the macroscopic efficiency negatively due to the bypassing of unswept sections in the reservoir. The most used or preferred WAG ratio is 1:1, as found in the literature [20]. The performance of different WAG ratios depends on many factors including fluid/rock interaction and their properties. Therefore, the best way to select WAG ratio is to carry out an optimization test. In most cases, the number of WAG cycles has a positive effect on oil recovery, which means that increasing the number of WAG cycles causes an increase in oil recovery.

Although the WAG process increases oil recovery significantly, it has the problem of late production which is economically unprofitable. Therefore, a new hybrid approach for enhanced oil recovery has been proposed, combining the LSW method with the WAG process to promote synergy of the mechanisms underlying these methods. Low-salinity, water alternating gas is a new EOR technique which combines the benefit of CO_2 WAG injection and LSW flooding to further enhance oil recovery and increase residual oil mobilization. Also, it uses the advantages of both methods to overcome the challenges associated with LSW and CO_2 WAG. It is economically viable since less CO_2 is required, compared to continuous CO_2 injection and no expensive chemicals are needed. In addition, the CO_2 produced can be re-injected and stored in the reservoir.

Teklu [22] conducted experimental work to prove the efficiency of LSWA CO_2 on oil recovery in different carbonate and sandstone samples. A clear reduction in the contact angle was observed at different wetting states, from a strong oil-wet state to water-wet state. Moreover, they reported that introducing CO_2 to the sea water at atmospheric pressure and room temperature, reduces IFT between oil and water and an even further reduction was obtained at reservoir pressure and temperature, as reported by Yang et al. [23]. Also, a core flooding experiment was performed on low permeability sandstone core after two weeks of aging. The injection sequence was seawater followed by LSW followed by immiscible CO_2. An additional 38.5% of oil was recovered by immiscible CO_2 flooding after the LSW flooding.

In 2016, Kumar et al. [24] conducted core flooding tests in the immiscible condition on low permeability sandstone, saturated by heavy oil (API = 29). They injected LSW (5000 ppm NaCl solution) alternating immiscible CO_2 with 1:1 WAG ratio. More than 65% of oil in place was recovered after the process.

Another recent work on LSWA CO_2 injection in sandstone was conducted by R. Ramanathan [25]. Core flooding tests were performed on aged Grey Berea sandstone. They examined the effect of brine salinity in the WAG process by using SW (TDS = 54,670 ppm) and NaCl solution (TDS = 5000 ppm). They found that approximately 76.1% total oil in place was recovered during injection of SW alternating immiscible CO_2. In contrast, LS alternating immiscible CO_2 resulted in 97.7% recovery. Teklu et al. [26] showed that a hybrid EOR process produced incremental oil up to twenty-five percent beyond seawater flooding at core-scale.

A literature review of laboratory works and simulation studies proved the efficiency of LSW, miscible CO_2-WAG and immiscible CO_2-WAG on different core characteristics and working conditions. However, there is no comprehensive study on the effect of smart water on LSWA CO_2 injection, especially for sandstones. Only the effect of dilution was observed in this process, while the impact of changing ionic composition on the performance of LS-immiscible-WA CO_2 has not yet been studied. It would be economically worthwhile to perform further investigation and experimental work to confirm the efficiency of the smart water, alternating gas injection technique on the improvement of oil recovery before field implementation. In this paper, a comprehensive study is performed to investigate the best scenario for LSWA CO_2 injection in sandstone and also the mechanism of LSWA CO_2 injection to increase oil recovery. Core flooding tests have been carried out to study the performance of different smart brines during the LSWA CO_2 EOR approach. Different studies on topics such as contact angle measurements, IFT measurements, and CO_2 solubility in brine and crude oil have been undertaken to analyze the mechanism of the proposed method.

2. Material and methodology

2.1. Rock and fluids

The formation brine (FB) was from a sandstone field in Oman. Smart brine samples were provided as per Table 1.

The density of the brines were obtained using an Anton Par densitometer (model DMA 4500 M) and the viscosity was measured using a Cannon Fenske viscometer at a temperature of T = 60 °C and atmospheric pressure. Table 2 summarizes the brine properties.

Light oil was provided from the same field with an API of 43, molecular weight of 209.4, and composition shown in Table 3.

Berea sandstone cores were used for the experiments. Table 4 summarizes the properties of the cores used. Porosity was measured using a Helium porosity meter while permeability was found using a gas permeability meter.

2.2. Methodology

2.2.1. CO_2 solubility in oil and brine

The solubility of CO_2 in crude oil and at different brine salinities was measured under room temperature and a pressure of 500 psi. The schematic diagram of the experimental apparatus used is illustrated in Fig. 1. It consists of a high pressure CO_2 cylinder which

Table 1
Composition of synthetic brines.

Salt type	FB (ppm)	Smart1 (ppm)	Smart2 (ppm)	Smart3 (ppm)
NaCl		5000	–	–
$MgCl_2.6H_2O$		–	5000	–
KCl		–	–	5000
TDS	50,000	5000	5000	5000

Table 2
Brine properties.

Brine	Density (g/cm^3)	Viscosity (cp)	PH
FB	1.136	0.707	4.12
SM1	0.999	0.479	6.50
SM2	0.977	0.490	6.49
SM3	1.101	0.452	5.90

is connected to an oil piston accumulator. The piston accumulator contains 50 ml of oil or 100 ml of brine, pressurized with 500 psi CO_2 gas. The pressure decay was recorded over a 30 min period. The final pressure and temperature were recorded when the system reached an equilibrium state. The CO_2 solubility in oil and different brine salinities was calculated using mass balance and ideal gas equations, where the solubility of CO_2 in oil (X_{co2}) was defined as the ratio of the total mass of CO_2 dissolved in 100 g of the original oil:

$$x_{co2} = \frac{m_{dis}}{m_{oil}} \times 100 \quad (1)$$

Where m_{oil} is the mass of the oil sample in grams ($\rho_o V_{o,i}$), and m_{dis} is the mass of CO_2 dissolved in oil in grams and calculated as:

$$m_{dis} = m_{CO2,i} - m_{Co2,f} \quad (2)$$

$$m_{dis} = \left(\frac{PV_{CO2} - M_{CO2}}{ZRT}\right)_i - \left(\frac{PV_{CO2} - M_{CO2}}{ZRT}\right)_f$$

$$m_{dis} = \frac{M_{CO2}V_{CO2}}{ZRT}\left\{\left(\frac{P}{RT}\right)_i - \left(\frac{P}{RT}\right)_f\right\}$$

Where:

$m_{CO2,i}$ and $m_{CO2,f}$ are the initial and final mass of CO_2 in grams,
P_i and P_f are the initial and final pressure in psi,
T_i and T_f are the initial and final temperature in Kelvin,
R is the universal gas constant (8.314 J/mol K),
Z is the g as compressibility factor,
V_{CO2} is the volume of CO_2 in cm^3,
M_{CO2} is the CO_2 molecular weight (44.01 g/mole),
$V_{o,i}$ is the initial oil volume in cm^3.

2.2.2. Core flooding experiment

The schematic setup of the core flooding system is shown in Fig. 2. It consists of a core holder (to hold 1.5″ diameter core plugs up to 7500 psi), a syringe pump to inject fluid, three piston accumulators to hold injection fluids (oil, brine and CO_2), a constant temperature air bath to hold the temperature up to 200 °C, a back pressure regulator to maintain system pressure up to 5000 psi, a hydraulic hand pump to apply confining pressure to the core holder, a precise Isco syringe pump (model 500D) to inject at a constant flow rate at high pressure, and differential pressure transducers installed in the inlet and outlet of the core holder to record injection and production pressures. A burette was used to collect the fluid produced at the outlet.

Table 3
Composition of the crude oil.

Carbon#	Wt.%	Carbon#	Wt.%
C12	23.719	C26	0.738
C14	35.215	C28	0.506
C16	21.474	C30	0.376
C18	6.998	C32	0.302
C20	7.006	C36	0.142
C22	2.371	C40	0.112
C24	1.039		

Table 4
Properties of the Berea sandstone cores.

Core#	Sample diameter (cm)	Sample length (cm)	Bulk volume (ml)	Dry weight (g)	Porosity, %
1	3.81	7.52	85.73	179.48	21.07%
2	3.81	7.5	85.51	179.11	20.57%
3	3.8	7.41	84.04	175.43	20.85%

Core samples were soaked in formation brine under vacuum for one day, to build up ionic equilibrium. Then, the weight of the wet cores was measured after saturation. The porosity and pore volume were calculated by dry and wet weight and the density of formation brine at reservoir temperature. Cores were held in the core holder at reservoir temperature for one day. Then, formation brine was injected at rates of up to 0.24 cc/min to ensure 100% brine saturation. The pressure drop was checked at each injection rate until it reached a steady state condition. The slope of the pressure drop versus injection rate was used to obtain absolute permeability by Darcy's law as follows:

$$Q = \frac{60kA(DP)}{14.69 \times 1000\mu L} \quad (3)$$

$$Kabs = \frac{Slope \times 14.69 \times 1000 \times \mu L}{60A} \quad (4)$$

where;

Q = Flow rate in cc/sec
Kabs = Absolute Permeability in mD
A = Cross sectional Area in cm^2
DP = Differential Pressure in psi
μ = Brine viscosity in cP
L = core length in cm

The calculated porosity, fluid permeability and pore volume are outlined in Table 5.

Cores were flooded by formation brine to ensure 100% water saturation, followed by crude oil to obtain initial oil saturation S_{wi}. Then, the cores were aged in crude oil for one month at a reservoir temperature of 60 °C, to restore initial wettability.

2.2.3. Contact angle (CA) measurement

Contact angle measurement was performed on sandstone discs to determine wettability alteration by different brine solutions.

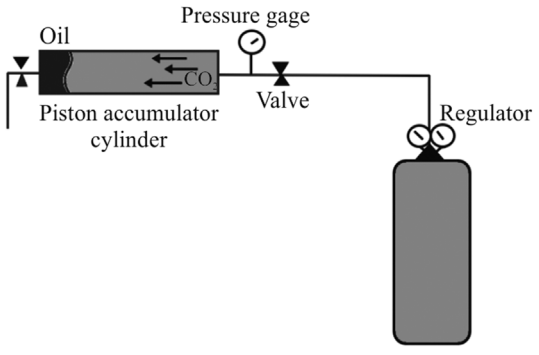

Fig. 1. Schematic of CO2 solubility in oil measurement apparatus.

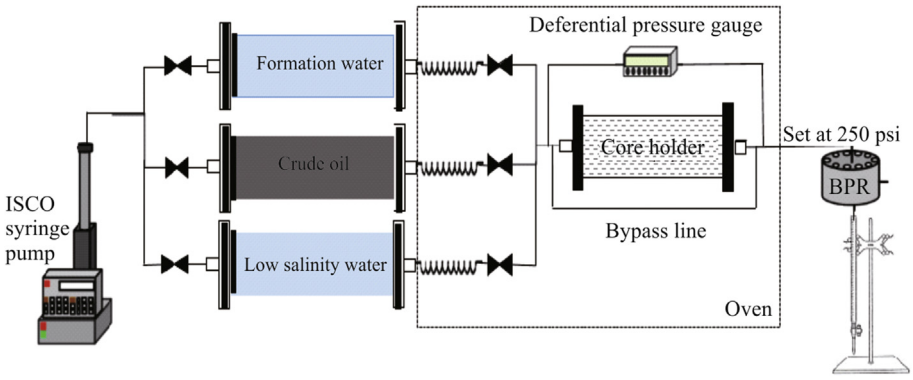

Fig. 2. Schematic diagram of core flooding setup.

Table 5
Core flooding test basic parameters.

	Core#1	Core#2	Core#3
Total volume (cm^3)	85.73	85.51	84.04
Cross sectional area (cm^2)	11.4	11.4	11.3
Porosity (%)	21.07	20.57	20.85
Permeability (k_{abs})	88.61	90.35	90.19
Pore volume (PV)	16.64	16.94	16.56
S_{wi}	0.439	0.419	0.423
S_{oi}	0.561	0.581	0.577

Initially, three discs were polished using sandpaper to obtain smooth surfaces. Then, each disc was soaked in formation brine for 2 h. Thereafter, they were aged in crude oil at reservoir temperature for three weeks to restore original wettability. Prior to CA measurement, the discs were washed in toluene and methyl cyclohexane to remove the oil from the surface and then they were soaked in different brines for two weeks. The device used to measure the angle between oil droplet and the aged disc surface at different locations is shown in Fig. 3.

A Spinning Drop Tensiometer (SDT) was used to measure the interfacial tension in the oil/brine systems.

3. Results and discussion

This section presents the results of core flooding, CO_2 solubility in oil and brine, IFT, CA and Z-potential. Our results were studied to provide a comprehensive analysis of the mechanisms underlying the CO_2 LSWAG process.

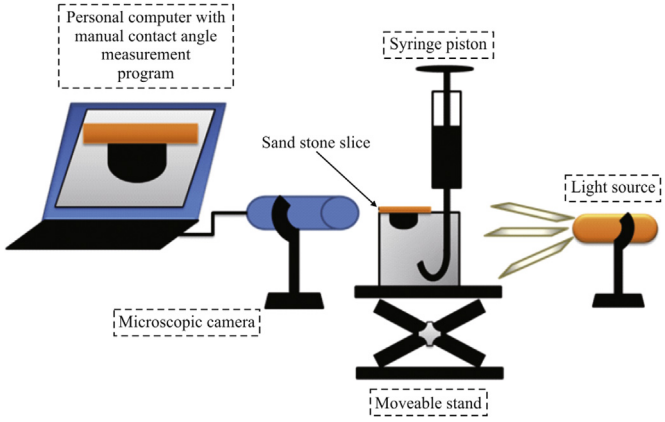

Fig. 3. Schematic diagram of the contact angle measurement system.

Three core flooding experiments were performed on three similar Berea sandstone core samples, to minimize variations in experimental conditions. The connate water saturation was obtained by material balance. The end-point relative permeability to oil at connate water saturation was found at four injection rates (1.50 cc/min, 1.25 cc/min, 1.00 cc/min and 0.75 cc/min) in order to achieve consistency in K_{ro} during the three experiments. Table 6 shows the saturation and permeability values obtained from the experiments. After 30 days of aging in oil at 60 °C, each core was flooded by a base brine of 50,000 ppm salinity at an injection rate of 0.24 cc/min. During the initial stage of water flooding, the pressure drop across the core started to build up steadily and then stabilized at around 3.60 psi after water breakthrough. The value of residual oil saturation after water flooding (S_{orw}) was found from the material balance for each experiment.

Five injection rates were used to determine the end-point relative permeability to water at residual oil saturation (0.24 cc/min, 0.44 cc/min, 0.68 cc/min, 0.84 cc/min and 1.08 cc/min), to ascertain the consistency in K_{rw} during each experiment. The recovery factor for all experiments is shown in Table 6.

3.1. Tertiary CO_2- LSWAG

Three different smart waters were used to test the effects of monovalent and divalent cations on oil recovery in the Tertiary CO_2 LSWAG approach. 5000 ppm NaCl, 5000 ppm $MgCl_2$ and 5000 ppm KCl samples were used. All experimental conditions were similar, maintaining a confining pressure of 1000 psi, a back pressure of 500 psi and a reservoir temperature of 60 °C to obtain immiscible CO_2 injection conditions, since the MMP of CO_2 on used oil was found to be greater than 2000 psi.

3.1.1. Experiment 1

Core #1 was used for this experiment (see Table 5). The pore volume was calculated to be 16.64 cc. The flood sequence was: formation brine of 50,000 ppm salinity followed by immiscible CO_2-alternating-5000 ppm NaCl low salinity water (LS1). The injection rate during high salinity waterflooding was 0.24 cc/min, to mimic Darcy velocity of 1 ft/day in the reservoir. CO_2 and LS1 were

Table 6
Secondary water flooding results.

Exp.#	K_{abs} (mD)	S_{wc}	$(S_{or})_{wf}$	RF_{wf} (OOIP)
1	88.6	0.44	0.380	0.322
2	90.3	0.42	0.408	0.297
3	90.2	0.42	0.399	0.309

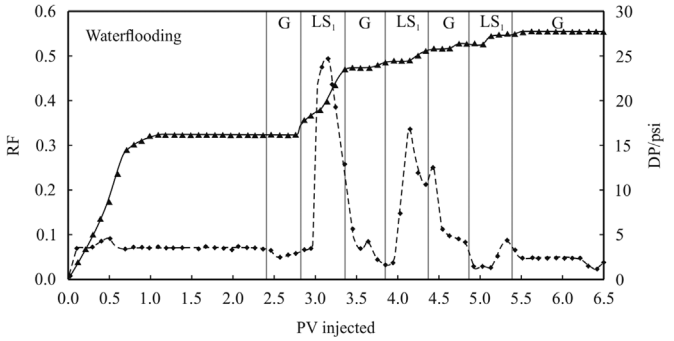

Fig. 4. Oil recovery (solid line) and pressure drop (dashed line) across the core in Exp. 1.

injected alternately, at a rate of 0.5 cc/min and slug size of 0.5 PV for each cycle. Three WAG cycles were performed and followed by a 1 PV continuous CO_2 injection.

Fig. 4 shows oil recovery (RF) and pressure drop (ΔP) across the core as a function of the pore volume injected. During waterflooding, 32% of oil was recovered during the first 1 PV water injection. No more oil recovery was observed after an additional 1.5 PV injection. The first slug of CO_2 and LS1 recovered 4% and 11% OOIP, respectively. The second slug of CO_2 recovered 2% OOIP and the second slug of LS1 recovered another 3% OOIP. The third cycle of injection yielded 3% OOIP and 1% OOIP was recovered during the last continuous slug of CO_2. The last additional slug of CO_2 was injected to make sure that the residual oil saturation was reached and no more oil recovery would be obtained by this process. A total recovery of 55.4% oil in place was obtained after a total 5.6 PV injection in the secondary and tertiary flooding stages.

3.1.2. Experiment 2

The conditions for this experiment were similar to Experiment 1 but it was performed on core #2. The calculated pore volume was 16.94 cc. The sequence of flooding was: 50,000 ppm high salinity water followed by immiscible CO2-alternating-5000 ppm $MgCl_2$ (LS2) with the injection rate similar to Experiment 1. Fig. 5 presents the oil recovery and pressure drop. 29.7% OOIP was recovered during waterflooding. The injection was terminated after 2.5 PV of water injection was achieved as no additional oil was produced. Three 1:1 WAG cycles were conducted with a total slug size of 1 PV in each cycle. The first slug of CO_2 recovered 1% OOIP while the first slug of LS2 produced 8% of OOIP. The second slugs of CO_2 and LS2 injection yielded 3% and 1% OOIP, respectively. An incremental oil recovery of 2% OOIP was recovered during the third cycle. The last continuous slug of CO_2 yielded 1% OOIP and there was no further oil production. Overall recovery was 45% OOIP after both

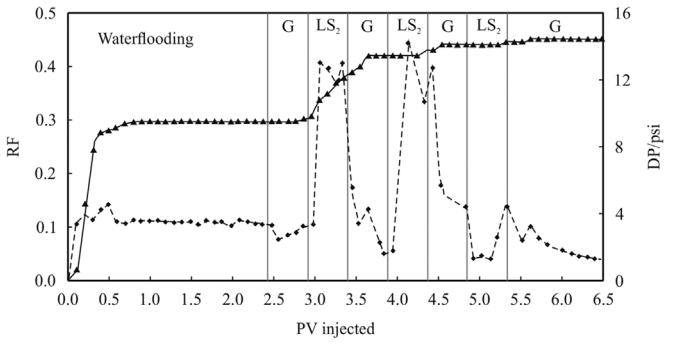

Fig. 5. Oil recovery (solid line) and pressure drop (dashed line) across the core in Exp. 2.

waterflooding and the WAG processes.

3.1.3. Experiment 3

The same procedure was applied to core #3. The brine used in the WAG process was 5000 ppm KCl (LS3). During 2.5 PV of waterflooding, the recovery factor was 30.9% OOIP, while 12.6% additional oil was obtained during the three cycles of immiscible CO_2-alternating-LS3 injection. Fig. 6 shows oil recovery and pressure drop across the core. Table 7 presents the results of the three tests in more detail. Our results show that oil recovery increases by 23%, 15.3% and 13% during the injection of 3 PV for SW1, SW2 and SW3, respectively. Therefore, our works prove the effectiveness of this hybrid process on oil recovery.

There was a continuous fluctuation in pressure drop across the core during immiscible CO2-alternating-low salinity water injection in all three experiments. SEM images and XRD show clear evidence of fines migration due to the presence of a high percentage of loose kaolinite clay, which tends to be mobilized during the injection of low salinity water, leading to a higher pressure drop. Fig. 7 illustrates the kaolinite particles, taken from SEM images.

3.2. Effect of CO_2 solubility in oil and brine on oil recovery improvement

Injection of CO_2 (either continuously or alternating with other fluids) efficiently enhances oil recovery, particularly in light to medium oil reservoirs, due to reductions in oil viscosity, better

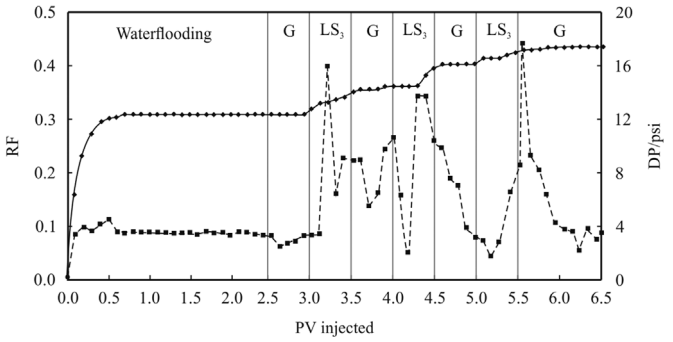

Fig. 6. Oil recovery (solid line) and pressure drop (dashed line) across the core in Exp. 3.

Table 7
Summary of the three conducted tests.

Test	Slug No.	Slug Type	Incremental Oil Recovery (%OOIP)	Total Oil Recovery (%OOIP)
NaCl-CO_2	1	CO_2	4	4
		LS_1	11	15
	2	CO_2	2	17
		LS_1	3	20
	3	CO_2	1	21
		LS_1	2	23
$MgCl_2$-CO_2	1	CO_2	1	1
		LS_2	8	9
	2	CO_2	3	12
		LS_2	1	13
	3	CO_2	1	14
		LS_2	1	15
KCl-CO_2	1	CO_2	2	2
		LS_3	3	5
	2	CO_2	1	6
		LS_3	4	10
	3	CO_2	1	11
		LS_3	2	13

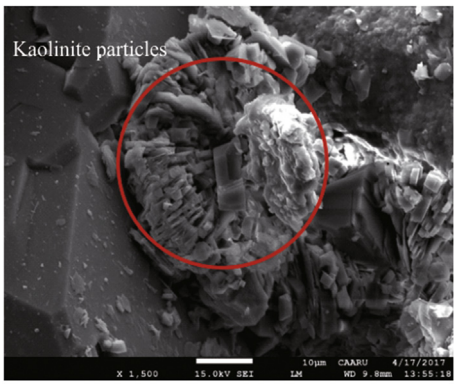

Fig. 7. SEM image showing kaolinite particles.

Table 8
Calculated mobility ratio during injection of LSWACO_2.

Test	Mobility ratio
CO_2-SW1	0.96
CO_2-SW2	1.21
CO_2-SW3	1.11

controlled mobility, increased oil swelling, minimized gravity segregation, and wettability alteration. Our results show that CO_2 stabilizes the displacement front of the water by mobility control during LSWACO_2 injection. Table 8 shows the mobility ratio during three core flooding tests. The values of mobility ratio, M, are close to 1 which represents stable displacement.

A pressure decay test was conducted to measure the solubility of CO_2 in oil. CO_2 was injected into an oil accumulator at a pressure of 500 psi. Then, it was terminated, pressure declined due to the solubility of the gas in the liquid. This pressure decay was recorded over time until it reached a stabilized state. Fig. 8 shows recorded pressure versus time for the oil/gas test. The solubility of CO_2 in oil was calculated using ideal gas and mass balance as shown in Equations (1) and (2). The molar solubility of CO_2 (mole of CO_2/mole of oil) was 0.348.

Solubility of CO_2 in oil increases at higher pressures. In our test, CO_2 was subcritical, since the working temperature was 22 °C which is less than the critical temperature of CO_2 ($T_c = 31.1$ °C). The experimental conditions were chosen in order to confirm that CO_2 is soluble in crude oil in the gaseous phase, rather than the liquid or supercritical phase. Our results agree with Al-Riyami's works [27]. She used a similar oil composition and API and found that CO_2 solubility in oil is around 0.412 mol of CO_2/mole of oil.

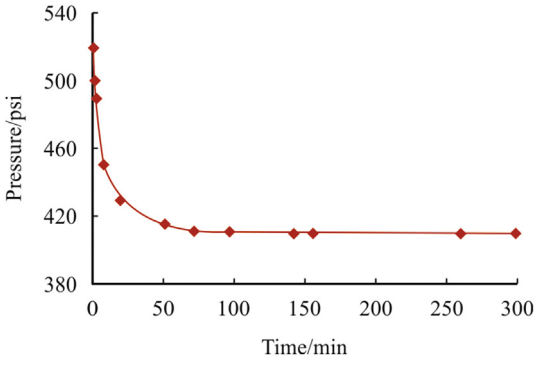

Fig. 8. Pressure decay during CO_2 solubility in oil test.

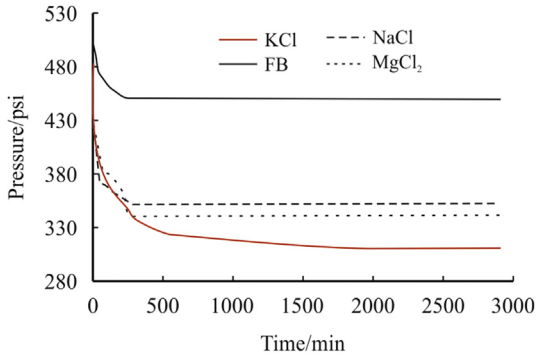

Fig. 9. Results of pressure decay test of CO_2 solubility in different brines.

CO_2 solubility was also measured in different brine compositions, in a similar way to the case of oil (by pressure decay testing). Fig. 9 represents the obtained pressure decay trend for different brine salinity at a temperature of T = 22 °C and initial pressure of P = 520 psi. It is obvious that CO_2 solubility increases as brine salinity decreases. A similar observation was obtained by Mosavat and Torabi [28]. They interpret this drop in CO_2 solubility as being a 'salting out' phenomenon. The salting-out effect states that, as the number of free ions in pure water increases, the number of water molecules available to interact with CO_2 decreases. This occurs because free ions undergo a hydration process with the existing water. As the radius of the ions increases, the hydration process increases and CO_2 solubility decreases. In our case, Mg^{2+} has the smallest radius, followed by Na^{+} and K^{+}. Consequently, the maximum solubility of CO_2 in brine was obtained by SW2. The measured CO_2 solubility for different brine salinities is shown in Table 9.

3.3. *Effect of different brine salinity and CO_2 on wettability alteration*

The wetting state of a rock surface is affected by temperature, brine salinity, pH of the connate water and injected brine, mineralogy of the rock surface, crude oil content in the reservoir, and gas in solution. In our tests, a reduction in pH was observed during increasing solubility of CO_2 in different brines, as shown in Table 10.

Table 9
Measured CO_2 solubility in different brine compositions.

Brine composition	Molality (mole of CO_2/Kg of brine)
High salinity brine	0.338
5000 ppm NaCl	0.703
5000 ppm $MgCl_2$	0.775
5000 ppm KCl	0.888

Table 10
PH of brines before and after CO_2 injection at a temperature of T = 22 °C and a pressure of P = 520 psi.

Sample number	Brine	pH	Reduction in pH
1	HS (50,000 ppm)	4.12	0.15
2	HS-CO_2	3.97	
3	NaCl (5000 ppm)	6.50	2.63
4	NaCl-CO2 (5000 ppm)	3.87	
5	KCl (5000 ppm)	5.90	2.25
6	KCl-CO_2 (5000 ppm)	3.65	
7	MgCl2 (5000 ppm)	6.49	2.93
8	MgCl2-CO2 (5000 ppm)	3.56	

Table 11
Values of CA and wettability alteration index for different treatments.

Sample number	Brine	Initial contact angle after aging in the base brine	Original contact angle after aging in the oil	Final contact angle after treatment	WI
1	HS (50,000 ppm)	51.24	118.19	71.43	0.70
2	HS-CO_2	51.24	114.33	42.12	1.14
3	NaCl (5000 ppm)	51.24	133.85	36.44	1.18
4	NaCl-CO_2 (5000 ppm)	51.24	118.78	33.34	1.27
5	KCl (5000 ppm)	51.24	109.45	41.95	1.16
6	KCl-CO_2 (5000 ppm)	51.24	122.33	43.58	1.11
7	$MgCl_2$ (5000 ppm)	51.24	126.21	52.37	0.98
8	$MgCl_2$-CO_2 (5000 ppm)	51.24	101.23	35.26	1.32

Eight brine samples were collected to study the contact angle (CA) between rock, brine and oil and to analyze the effect of gas injection on wettability alteration. Disc of samples initially were saturated with base brine to obtain initial wetting state. The average initial contact angle of the used samples was around 51.24° which reflects a preferentially water-wet state. Then, they were aged in crude oil at 60 °C for two weeks to restore original wettability. After two weeks of aging in crude oil, contact angle increases towards an intermediate state due to partial adsorption of the polar components of crude oil on clay surfaces. The CA values are shown in Table 11. However, the contact angle was reduced towards a more water-wet state after aging in different brine samples. Fig. 10 and Table 11 show CA values after aging in different brines. A sample of the initial CA was shown in Fig. 11Fig. 11 Comparing the wettability index (WI) (Fig. 12 and Table 11) helps us to better understand wettability alteration by LS and CO_2. Wettability index was defined as

$$WI = \frac{\theta_{original} - \theta_{final}}{\theta_{original} - \theta_{initial}} \quad (5)$$

where,

$\theta_{original}$ is the obtained CA after aging samples in crude oil.
$\theta_{initial}$ is the obtained CA after aging samples in base brine.
θ_{final} is the obtained CA after aging samples in different brine salinities.

Hence, WI equal to one means that the treatment changes the wettability to the initial water wet condition before aging with oil. WI greater than one means more water wetness compared to the initial condition.

The decrease in CA after aging in different brine samples is due to the multicomponent ion exchange mechanism (MIE). Cations are exchanged based on their different affinity towards clay surfaces. The relative replacement power of cations at room temperature is stated by Ole Martin Valderhaug [26] as:

$Li^+ < Na^+ < K^+ < Mg^{2+} < Ca^{2+} < Sr^{2+} < Ba^{2+} < H^+ < Al^{3+}$

Although Mg^{2+} has the highest affinity towards clay surfaces, compared to K^+ and Na^+, it has a lower wettability alteration index

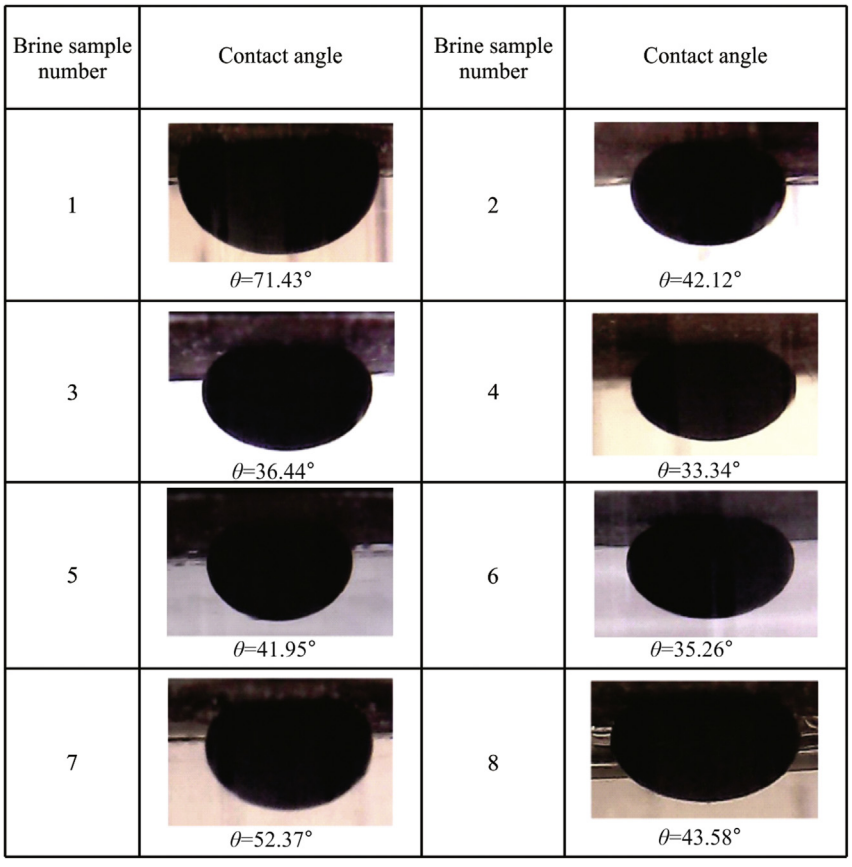

Fig. 10. Captured photos of CA after aging in different brine samples.

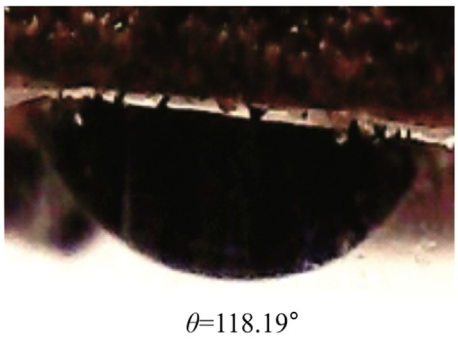

Fig. 11. A sample of captured photo of CA after aging in oil as the initial condition.

(as Mg^{2+} tends to form a bridge with the crude oil, unlike K^+ and Na^+). Bridging with crude oil mainly occurs in the presence of a divalent cation, such as Mg^{2+} and Ca^{2+}. Since HS solution has a high concentration of divalent ions, the bridging process is more prevalent, therefore it shows the lowest WI value. WI even gets higher when the pH of the brine solutions was lowered in the presence of CO_2. Presence of H^+ promotes the MIE mechanism, since the affinity of H^+ towards clay surfaces is higher than Mg^{2+}, K^+, and Na^+.

The monovalent NaCl solution gave the highest oil recovery compared to KCl and $MgCl_2$ solutions. This can be interpreted by the MIE mechanism as Na^+ replacing and substituting the divalent ions and Mg^{2+} and Ca^{2+} cations. Therefore, the maximum reduction in residual oil saturation by immiscible CO_2-aternating low salinity water was obtained by NaCl solution. The reduction in S_{or} was 12.90%, 8.85% and 7.25% for LS1, LS2 and LS3 giving an additional recovery of 23.0%, 15.3% and 12.6% OOIP, respectively. Monovalent KCl solution yielded the least oil recovery during the tertiary flood. The only reasonable attribution is that the formation clay may not have readily accepted K^+, as it did with Na^+. A similar conclusion was obtained by Kumar et al. [8].

3.4. Effect of different brine salinity and CO_2 on IFT measurement

As the IFT between injected brine and oil reduces, capillary pressure decreases, enhancing oil displacement. Eight experiments were performed to investigate the effect of reducing brine salinity, changing cation type, and changing pH due to the presence of CO2 on IFT. IFT between each sample and crude oil was measured at a temperature of 60 °C and the results are shown in Table 12.

High salinity brine and $MgCl_2$ solution have the highest IFT, as these brines contain divalent ions that disturb the hydrogen bond between the negatively charged, polar component of crude oil and the partially positively charged hydrogen atom in the water molecules. Disruption of the hydrogen bond at the oil/brine interface occurs due to the salting-out effect, which reduces the solubility of organic components in water and increases IFT. During the salting-out mechanism, the solubility of a nonelectrolyte substance in water decreases when the salt concentration increases in the brine. Introducing CO_2 has an advantage in reducing IFT between CO_2 saturated brine and crude oil. However, changes in the IFT of smart brines are not noticeable, which means that IFT alteration is not a dominant mechanism in this process.

Table 12
IFT values between crude oil and brine samples before and after introducing CO_2.

Brine Sample	IFT (mN/m)
HS (50,000 ppm)	22.57
HS-CO_2	18.22
NaCl (5000 ppm)	17.93
NaCl-CO_2 (5000 ppm)	13.66
KCl (5000 ppm)	19.00
KCl-CO_2 (5000 ppm)	16.73
$MgCl_2$ (5000 ppm)	20.08
$MgCl_2$-CO_2 (5000 ppm)	13.95

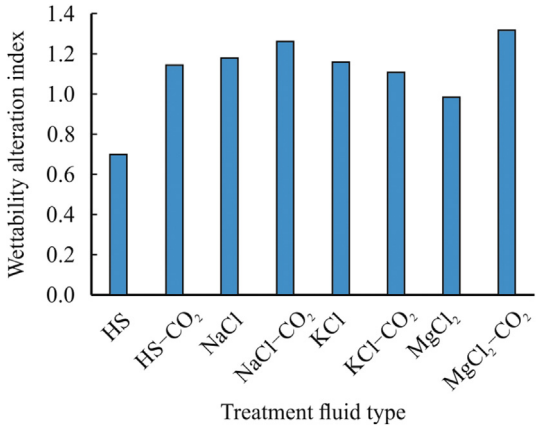

Fig. 12. Wettability index alteration before and after gas injection.

4. Conclusions

Low salinity water-flooding is an emerging EOR technique that mainly influences the interactions occurring in crude oil-brine-rock (CBR) systems. The WAG process is a well-accepted and proven EOR method which plays an important role in stabilizing the displacement front of the injected fluid through mobility control, thereby enhancing oil recovery. Therefore, combining the two processes as low salinity water-alternating-CO_2 injection can further enhance oil recovery by promoting the mechanisms underlying each process. Our research focussed on studying the performance of LSWA CO_2 on oil recovery in sandstone reservoirs and the impact of using smart water instead of diluted brine on oil recovery enhancement.

Different laboratory tests were performed to prove the viability of LSWA CO_2 on oil recovery and to come up with clear justification regarding the mechanisms behind this EOR technique. Three smart brine solutions (besides high salinity brine) were used to study the effect of changing the type of cation dissolved in low salinity water; these were: 5000 ppm NaCl (SW1), 5000 ppm $MgCl_2$ (SW2), and 5000 ppm KCl (SW3). The following conclusions can be drawn, based on the results obtained:

(1) Tertiary low salinity water-alternating immiscible CO_2 (LSWA CO_2) injection produced significant incremental oil recovery. SW1 resulted in higher additional oil recovery compared to SW2 and SW3.
(2) HS and SW1 yielded lower CO_2 solubility in brine, thus higher CO_2 solubility in the crude oil which promotes oil swelling and oil viscosity reduction.
(3) A favorable wettability alteration was achieved by SW1 and SW3 followed by SW2. SW1 and SW3 contain monovalent cations that tend to replace divalent cations, that are initially presented in the connate water, to achieve thermodynamic equilibrium at the brine/rock and brine/oil interfaces.
(4) Injection of CO_2 showed a positive effect on oil recovery during LSWAG injection in sandstones. It controlled the displacement front of the injected fluid through mobility control. Also, further wettability alteration was obtained with CO_2 injection.

(5) Dissolution of CO_2 in the studied smart water lowered the interfacial tension between CO_2-saturated brine and crude oil but the dominant mechanisms for the LSWA CO_2 technique are wettability alteration due to multicomponent ionic exchange (MIE) and partial miscibility of CO_2.

References

[1] N.R. Morrow, Wettability and its effect on oil recovery, J. Petrol. Technol. 42 (12) (1990) 1–476.

[2] P.L. McGuire, J.R. Chatham, F.K. Paskvan, D.M. Sommer, F.H. Carini, Low salinity oil recovery: an exciting new EOR opportunity for Alaska's North Slope, in: SPE Western Regional Meeting, Society of Petroleum Engineers, 2005, January.

[3] C.T.Q. Dang, Mechanistic Modeling, Design, and Optimization of Low Salinity Waterflooding, 2015. Doctoral dissertation, University of Calgary).

[4] G.Q. Tang, N.R. Morrow, Influence of brine composition and fines migration on crude oil/brine/rock interactions and oil recovery, J. Petrol. Sci. Eng. 24 (1999) 2–4 pp.99–111.

[5] A. Hiorth, L.M. Cathles, M.V. Madland, The impact of pore water chemistry on carbonate surface charge and oil wettability, Transport Porous Media 85 (1) (2010) 1–21.

[6] H. Pu, X. Xie, P. Yin, N.R. Morrow, Low-salinity waterflooding and mineral dissolution, in: SPE Annual Technical Conference and Exhibition, Society of Petroleum Engineers, 2010, January.

[7] N. Morrow, J. Buckley, Improved oil recovery by low-salinity waterflooding, J. Petrol. Technol. 63 (05) (2011) 106–112.

[8] T. Austad, A. RezaeiDoust, T. Puntervold, Chemical mechanism of low salinity water flooding in sandstone reservoirs, in: SPE Improved Oil Recovery Symposium, Society of Petroleum Engineers, 2010, January.

[9] T. Austad, S.F. Shariatpanahi, S. Strand, C.J.J. Black, K.J. Webb, Conditions for a low-salinity enhanced oil recovery (EOR) effect in carbonate oil reservoirs, Energy Fuel. 26 (1) (2011) 569–575.

[10] A. Lager, K.J. Webb, C.J.J. Black, M. Singleton, K.S. Sorbie, Low salinity oil recovery-an experimental investigation1, Petrophysics 49 (01) (2008).

[11] A. Zahid, A.A. Shapiro, A. Skauge, January. Experimental studies of low salinity water flooding carbonate: a new promising approach, in: SPE EOR Conference at Oil and Gas West Asia, Society of Petroleum Engineers, 2012.

[12] S.Y. Lee, K.J. Webb, I.R. Collins, A. Lager, S.M. Clarke, M. O'Sullivan, A.F. Routh, Low salinity oil recovery–increasing understanding of the underlying mechanisms of double layer expansion, in: IOR 2011-16th European Symposium on Improved Oil Recovery, 2011, April.

[13] D.J. Ligthelm, J. Gronsveld, J. Hofman, N. Brussee, F. Marcelis, H. van der Linde, Novel waterflooding strategy by manipulation of injection brine composition, in: EUROPEC/EAGE Conference and Exhibition, Society of Petroleum Engineers, 2009, January.

[14] H. Mahani, A.L. Keya, S. Berg, W.B. Bartels, R. Nasralla, W.R. Rossen, Insights into the mechanism of wettability alteration by low-salinity flooding (LSF) in carbonates, Energy Fuels 29 (3) (2015) 1352–1367.

[15] R.A. Nasralla, H.A. Nasr-El-Din, Double-layer expansion: is it a primary mechanism of improved oil recovery by low-salinity waterflooding? SPE Reservoir Eval. Eng. 17 (01) (2014) 49–59.

[16] K.S. Sorbie, I. Collins, A proposed pore-scale mechanism for how low salinity waterflooding works, in: SPE Improved Oil Recovery Symposium, Society of Petroleum Engineers, 2010, January.

[17] G.Q. Tang, N.R. Morrow, Influence of brine composition and fines migration on crude oil/brine/rock interactions and oil recovery, J. Petrol. Sci. Eng. 24 (1999) 2–4 pp.99–111.

[18] I. Fjelde, S.M. Asen, A.V. Omekeh, Low salinity water flooding experiments and interpretation by simulations, in: SPE Improved Oil Recovery Symposium, Society of Petroleum Engineers, 2012, January.

[19] M.M. Kulkarni, D.N. Rao, Experimental investigation of miscible and immiscible Water-Alternating-Gas (WAG) process performance, J. Petrol. Sci. Eng. 48 (2005) 1–2 pp.1–20.

[20] E. Stenby, A. Skauge, J. Christensen, Review of WAG field experience, SPE Reservoir Eval. Eng. (2001) 1–10.

[21] J.P. Srivastava, L. Mahli, Water alternating gas (WAG) injection a novel EOR technique for mature light oil fields a laboratory investigation for GS-5C sand of gandhar field, in: A Paper Presented in Biennial International Conference and Exposition in Petroleum Geophysics, Hyderabad, 2012.

[22] T.W. Teklu, Experimental and Numerical Study of Carbon Dioxide Injection Enhanced Oil Recovery in Low-permeability Reservoirs, Colorado School of Mines, 2015.

[23] D. Yang, P. Tontiwachwuthikul, Y. Gu, Interfacial tensions of the crude oil+ reservoir brine+ CO2 systems at pressures up to 31 MPa and temperatures of 27 C and 58 C, J. Chem. Eng. Data 50 (4) (2005) 1242–1249.

[24] H.T. Kumar, A.M. Shehata, H.A. Nasr-El-Din, Effectiveness of low-salinity and CO2 flooding hybrid approaches in low-permeability sandstone reservoirs, in: SPE Trinidad and Tobago Section Energy Resources Conference, Society of Petroleum Engineers, 2016, June.

[25] R. Ramanathan, A.M. Shehata, H.A. Nasr-El-Din, Effect of rock aging on oil recovery during water-alternating-CO 2 injection process: an interfacial tension, contact angle, coreflood, and CT scan study, in: SPE Improved Oil Recovery Conference, Society of Petroleum Engineers, 2016, April.

[26] T.W. Teklu, W. Alameri, H. Kazemi, R.M. Graves, A.M. AlSumaiti, Low salinity water–Surfactant–CO2 EOR, Petroleum 3 (3) (2017) 309–320.

[27] S. Al Riami, Effect of Oil Type on Performance of Carbonated Water Injection (CWI) for Enhanced Oil Recovery under Consistent Operating Conditions, 2016. Msc Thesis, Sultan Qaboos University).

[28] N. Mosavat, F. Torabi, Performance of secondary carbonated water injection in light oil systems, Ind. Eng. Chem. Res. 53 (3) (2013) 1262–1273.